DOI: 10.31276/VJSTE.62(4).49-59

Using a numerical model with moving boundary conditions to study the bed change of a Mekong river segment in Tan Chau, An Giang, Vietnam

Kim Tran Thi[1, 2], Huy Nguyen Dam Quoc[1], Phung Nguyen Ky[3], Bay Nguyen Thi[4, 5*]

[1]*Ho Chi Minh city University of Natural Resources and Environment*
[2]*Institute for Environment and Resources, Vietnam National University, Ho Chi Minh city*
[3]*Institute for Computational Science and Technology*
[4]*Ho Chi Minh city University of Technology*
[5]*Vietnam National University, Ho Chi Minh city*

Received 11 August 2020; accepted 5 November 2020

Abstract:

Numerical models that calculate bed change are becoming increasingly popular because of their long-term forecast projections and their ability to identify causes of bed change. However, the reliability of the simulation results depends on the length of the data series and the algorithms in the model, in which the boundary condition method plays a critical role. The aim of this study is to assess the effectiveness of the HYDIST model to update wet and dry fronts as well as recalculate the wet boundaries of the hydraulic model before its input into the sediment transport model. The moving boundary theories (wet and dry fronts) of Zhao (1994) and Sleigh (1998) were applied. The velocity distribution of the wet boundaries was recalculated after every time step, then the outcomes of the hydraulic model were used as input for the sediment transport model. The results showed good agreement between the simulated and measured data in term of discharge, water level, and sediment concentration. At the same time, the HYDIST model can be successfully used to simulate sediment deposition and riverbank movement.

Keywords: **bed change, boundary condition, Mekong, numerical model, sediment transport.**

Classification number: **5.1**

Introduction

Sediment transport affects river environments in many ways via erosion and sediment deposition. The development and degradation of a riverbed significantly influence flow changes and the economic development of the region. Besides, a change in the river profile can threaten channel stability and affect irrigation facilities on both sides of the river. Therefore, the accurate simulation of bed change in a river is of great significance to regional planning and other long-term projects.

Today, with computer engineering and information technology development, researchers have built numerical models that can simulate changes in riverbeds. With the advantage of simulating many scenarios over different periods, identifying the cause of an impact and forecasting the future is possible. However, accurate calculations and long-term forecasts take a significant amount of time to calculate.

Sediments are solid mineral particles that are transported and deposited in the water flow resulting in their accumulation in riverbeds and floodplains. Sediments are usually formed as heterogeneous particles of various sizes with a larger specific gravity than water [1-3]. Based on the laws of motion, sediments are classified into suspended and bottom sediments [1-4]. The evolution of the loading or deposition of bed sediments changes the topography of the river bed and affects changes in river flows [5-7].

To simulate the change of the riverbed, scientists have used many methods such as observations, physical models,

* *Corresponding author: Email: ntbay@hcmut.edu.vn*

and numerical models. For simple curved channels, both physical models on the laboratory scale and large scale surveys have been used to study sediment transport [8-10]. However, numerical models pose major advantages in simulation and prediction [11-15].

For irregular topography, both positive and negative bed slopes generally exist and lead to cell drying and wetting with moving fronts, which cannot be easily solved by a simple horizontal boundary condition. Therefore, some techniques have been developed for these shallow water equations. Zhao, et al. (1994) [16] and Sleigh, et al. (1998) [17] introduced two similar schemes to track the wetting and drying fronts, in which cells are divided into wet, dry, and partially dry types according to two tolerances [16, 17]. Technology for tracking the wet-dry front has been developed, in combination with the method of Brufau, et al. (2004) [18], to achieve zero mass error by Liu, et al. (2014) [19].

Based on the above analysis, in this paper, we propose improving the HYDIST model initially developed by Bay, et al. (2012, 2019) [20, 21]. This study will focus on developing the boundary conditions in the hydraulic model and sediment transport model of the HYDIST model.

1. First, the moving boundaries problem (wetting and drying fronts), which is based on the work by Zhao, et al. (1994) [16] and Sleigh, et al. (1998) [17], is applied.

2. Secondly, the flow sequence, Q(t), and the velocity distribution on the liquid boundary, u,v(x, y, t), is recalculated according to the formula assuming the roughness coefficient n is constant at the boundary inlet [22], which are each applied to achieve zero error at the positions of the boundaries.

The developed model will be calculated for a segment of the Tien river located in Tan Chau town, and compared with observational data to assess the reliability of the model.

Materials and methods

Study area

Tien river is one of the two major tributaries of the Mekong delta (along with the Hau river) flowing into Vietnam (Fig. 1). After branching in Phnom Penh (Cambodia), the Tien river flows into Vietnam beginning in Tan Chau town, An Giang province. Then, the main flow goes through the provinces of An Giang, Dong Thap, Vinh Long, and Ben Tre [23].

A segment flowing through An Giang has the style of a braided river; the riverbed is wide with coastal sandbars and sand bars in the heart. This part has a complex terrain, is stream folded, and has intense erosion. In recent years, failure banks have increasingly affected the socio-economic development and planning in the local area and construction along the river in the An Giang province [24-27].

The topography was collected at the Department of Investment and Construction Project of the Tan Chau area on October 6, 1999. The features (water level ς (t), discharge Q(t), and total suspended sediment C(t)) at the Tan Chau station were collected from 1999 to 2006 from the Project: "Research to identify causes, mechanisms and propose feasible technical and economical solutions to reduce erosion, sedimentation for the Mekong river system (2017-2020)", code No. KHCN-TNB.DT/14-19/C10 in 2019.

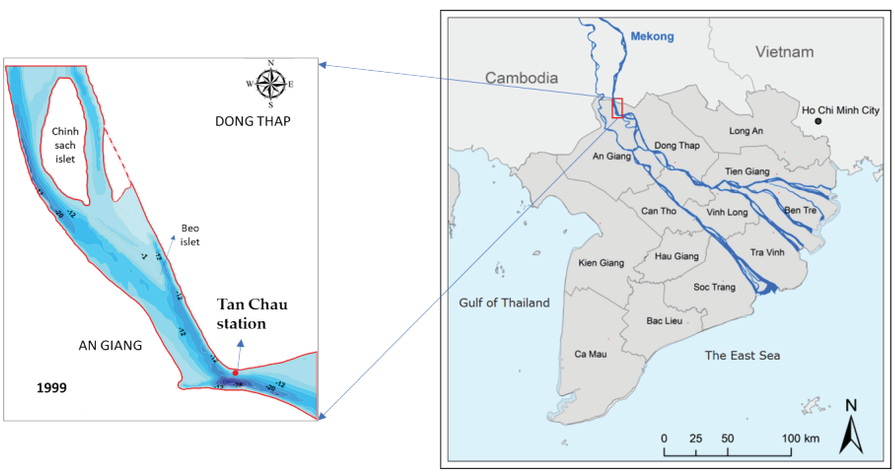

Fig. 1. Study area.

HYDIST model

The adopted model is a 2D surface model where Ox and Oy represent the length and width of the study area as seen in Fig. 2. The model is based on a system of four governing equations: the Reynolds equation in Ox and Oy directions, the continuity equation, the suspended sediment transport equation, and the bedload continuity equation as follows [21, 28].

Reynolds equation in Ox and Oy directions:

$$\frac{\partial u}{\partial t}+u\frac{\partial u}{\partial x}+v\frac{\partial u}{\partial y}=-g\frac{\partial \varsigma}{\partial x}-Ku\frac{\sqrt{u^2+v^2}}{h+\varsigma}+A\nabla^2 u \quad (1)$$

$$\frac{\partial v}{\partial t}+u\frac{\partial v}{\partial x}+v\frac{\partial v}{\partial y}=-g\frac{\partial \varsigma}{\partial y}-Kv\frac{\sqrt{u^2+v^2}}{h+\varsigma}+A\nabla^2 v \quad (2)$$

Continuity equation:

$$\frac{\partial \varsigma}{\partial t}+\frac{\partial}{\partial x}[(h+\varsigma)u]+\frac{\partial}{\partial y}[(h+\varsigma)v]=0 \quad (3)$$

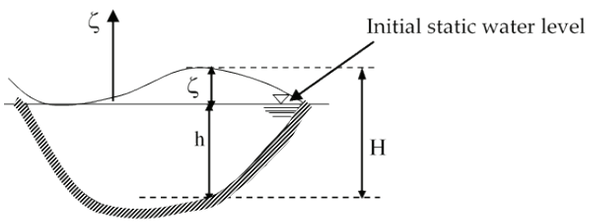

Fig. 2. The illustration of the initial static level.

Suspended sediment transport equation:

$$\frac{\partial C}{\partial t}+\gamma_v\left(u\frac{\partial C}{\partial x}+v\frac{\partial C}{\partial y}\right)=\frac{1}{H}\frac{\partial}{\partial x}\left(HK_x\frac{\partial C}{\partial x}\right)+\frac{1}{H}\frac{\partial}{\partial y}\left(HK_y\frac{\partial C}{\partial y}\right)+\frac{S}{H} \quad (4)$$

Bed load continuity equation:

$$\frac{\partial h}{\partial t}=\frac{1}{1-\varepsilon_p}\left[E+\frac{\partial}{\partial x}\left(HK_x\frac{\partial C}{\partial x}\right)+\frac{\partial}{\partial y}\left(HK_y\frac{\partial C}{\partial y}\right)+\frac{\partial q_{bx}}{\partial x}+\frac{\partial q_{by}}{\partial y}\right] \quad (5)$$

with $q_i=(b_y, b_{ee})$

$$q_b=0.053\left(\left(\frac{\rho_s}{\rho}-1\right)g\right)^{0.5}d_m^{1.5}T^{2.1}D_*^{-0.3}\frac{(u,v)}{\sqrt{u^2+v^2}} \quad (6)$$

Numerical approach

These equations are solved by the Alternating Direction Implicit (ADI) method. The fundamental concept of ADI is to split the finite difference equations into two, one with the x-derivative and the next with the y-derivative, both taken implicitly [29]. The computational grid for the governing system of equations is shown in Fig. 3.

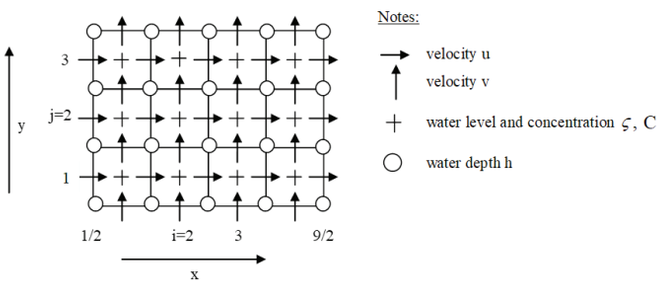

Fig. 3. Computational grid for the governing system of equations.

From the figure, the u, v, and ς components are specially arranged. In more detail, ς and C are placed at the centre of the grid cell (i, j), while u is placed in the position (i+1/2, j) and v is in the position (i, j+1/2) (with i, j = 1, 2, 3…). The width and height of a grid cell is Δx and Δy, respectively. The grid is numbered by the index i (for x directions) from 1 to N and the index j (for y) from 1 to M [21]. The model is calculated by three coupled equations: the Reynolds, continuity, and suspended sediment transport equations. At the first-half step, ς, u, and C are implicitly solved in the x-direction and v is the opposite. For the following half step, ς, v and C are implicitly solved in the y-direction and u is the opposite. The bedload continuity equation is solved alternately after a time step.

In this paper, the hydraulic and sediment transport boundaries are developed as follows.

Regarding the hydraulic model: the upstream boundary is the time-dependent sequence of flow data, Q(t), over the region, while the downstream boundary of the flow will be in the form of the fluctuating water level, ς(t). From the flow sequence Q(t), the program will recalculate the velocity distribution u,v(x, y, t) on the liquid boundary according to the formula assuming the roughness coefficient n is constant at the boundary inlet. Then, the boundary is calculated as follows [22]:

$$u,v=\left[\frac{Q}{\frac{\sum(h_i^{\frac{5}{3}})}{h_i\Delta x}}h_i^{\frac{5}{3}}\right] \quad (7)$$

where

Q=Q(t): the sequence of flow data (m^3/s);

h_i: bottom depth at calculation node (m);

Δx: the distance between two nodes (m).

Furthermore, because the fluctuations of water levels vary from time to time, the moving boundaries problem (flooding and drying fronts), which is based on the work by Zhao, et al. (1994) [16] and Sleigh, et al. (1998) [17], is applied in this model. The study area is classified into grid cells. The depth of each element/cell is monitored and the elements are classified as dry, partially dry, or wet. In more detail, an element is defined as flooded if the water depth of at least three corners of a grid cell is greater than 0.1. An element is dry if the water depth of at least 3 corners of a grid cell is less than 0.1, then, the element is removed from the calculation. An element is partially dry if the water depth at two corners of a grid cell is less than 0.1. These two parameters will regulate when a given cell should be exposed for a flooding or drying check during the simulation.

Figure 4 presents the general framework of the calculation for our coupled model based on the coupling of all the governing equations previously described. Hydrodynamic and sediment transport models were tested with an analytic solution [20].

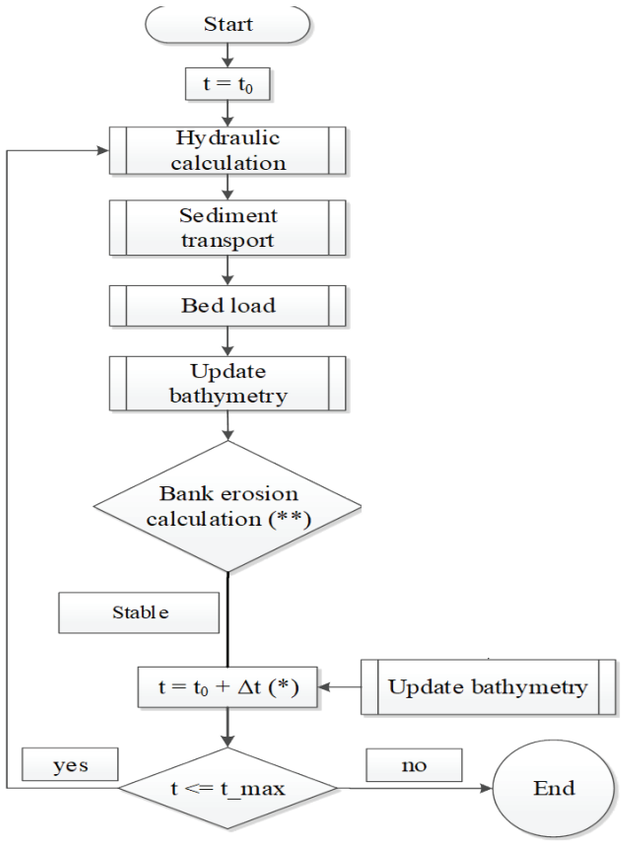

Fig. 4. General computational procedure used in the coupled.

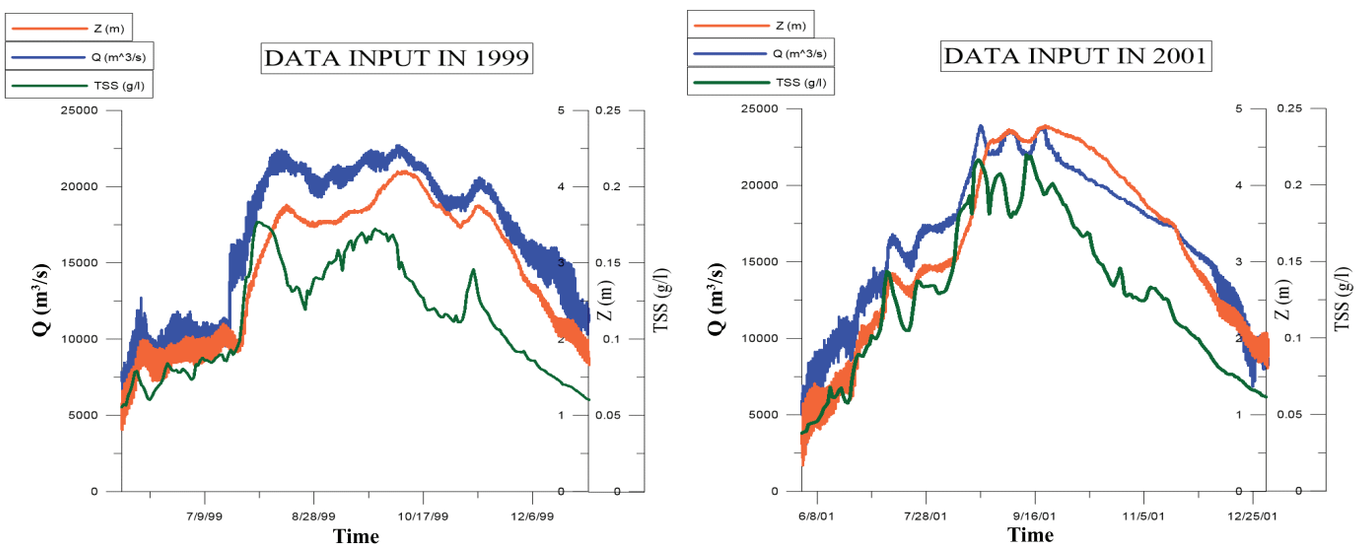

Fig. 5. Input data in 1999 and 2001.

Setup of the model for the study area

Bathymetry: the entire study area is represented by a rectangular mesh of size 981x845 pixels, including the land and riverbed, where $\Delta x=\Delta y=10$ m and the time step $\Delta t=2$ s. At the curve, the size is 492x424 pixels including the land and riverbed. The boundary condition includes the flow, Q(t), alluvial, C(t), and water level, ς(t), of the flood seasons from 1999 to 2006 at the Tan Chau station.

Initial conditions: from $t_0=0$ in the model, the hydraulic module is tied to a static state and the sediment transport module is set to an initial constant basal concentration. If the problem is calculated from a time $t=t_1$, the initial condition is the velocity fields u,v(x, y) and concentration C(x, y) at time t_1 across the computational domain.

Boundary conditions:

(1) Open boundaries: the Q(t), C(t), and ς(t) of the flood seasons from 1999 to 2006 at Tan Chau station (as Fig. 5). The study area has two boundaries whose features are identified based on the correlation functions f(ς), f(Q), and f(C) from the Tan Chau station. Measurement data at the boundaries of the project come from "Research to identify causes, mechanisms and propose feasible technical and economical solutions to reduce erosion, sedimentation for the Mekong river system (2017-2020)", code No. KHCN-TNB.DT/14-19/C10 from 10 am 06/06/2018 to 10 am 13/06/2018. Typical boundary data for 1999 and 2001 are shown in Fig. 5.

(2) Solid wall boundary: hydrodynamics conditions $u_n=0$ and sediment transport conditions $\frac{\partial C}{\partial n_p}=0$.

Model calibration and validation criteria

In order to calibrate and validate the model with a comparison, the Nash-Sutcliffe efficiency coefficient (NSE) and the coefficient of determination (R^2) are used to measure model performance [30-32].

The Nash-Sutcliffe efficiency coefficient (NSE): the NSE ranges between −∞ and 1. A value of NSE=1 indicates a perfect match between observed and predicted results. The general performance ratings for model evaluation are shown in Table 1. NSE is computed as shown in Eq. (8):

$$NSE = 1 - \left[\frac{\sum_{i=1}^{n}(O_i - P_i)^2}{\sum_{i=1}^{n}(O_i - \overline{O})^2}\right] \quad (8)$$

where

O_j: the ith observation for the constituent being evaluated;

P_i: the ith simulated value for the constituent being evaluated;

$\overline{O}$: the mean of observed data for the constituent being evaluated;

N: is the total number of observations.

Table 1. General performance ratings for model evaluation.

			Range	Optimal value	Performance Rating			
					Very good	*Good*	*Satisfactory*	*Unsatisfactory*
NSE	Flow	Annual	−∞ to 1.0	1.0	>0.75	0.60≤NSE≤0.75	0.50≤NSE≤0.60	≤0.50
		Monthly			>0.85	0.70≤NSE≤0.85	0.55≤NSE≤0.70	≤0.55
		Daily			>0.80	0.70≤NSE≤0.80	0.50≤NSE≤0.70	≤0.50
	Sediment				>0.80	0.70≤NSE≤0.80	0.45≤NSE≤0.70	≤0.45
	General				>0.80	0.60≤NSE≤0.80	0.50≤NSE≤0.60	≤0.50
R2	Flow	Annual	0.0 to 1.0	1.0	>0.75	0.70≤ R^2 ≤0.75	0.60≤ R^2 ≤0.70	≤0.60
		Monthly			>0.85	0.80≤ R^2 ≤0.85	0.70≤ R^2 ≤0.80	≤0.70
		Daily			>0.85	0.70≤ R^2 ≤0.85	0.50≤ R^2 ≤0.70	≤0.50
	Sediment				>0.80	0.65≤ R^2 ≤0.80	0.40≤ R^2 ≤0.65	≤0.40
	General				>0.80	0.70≤ R^2 ≤0.80	0.50≤ R^2 ≤0.70	≤0.50

The coefficient of determination (R^2)

The coefficient of determination, R^2, ranges between 0 and 1. It describes the portion of the variance in the measured data where higher values indicate less error variance. The general performance ratings for model evaluation using the coefficient of determination is shown in Table 1. R^2 is computed as shown in Eq. (9):

$$R^2 = \left[\frac{\sum_{i=1}^{n}(O_i - \overline{O})(P_i - \overline{P})}{\sqrt{\sum_{i=1}^{n}(O_i - \overline{O})^2}\sqrt{\sum_{i=1}^{n}(P_i - \overline{P})^2}}\right]^2 \quad (9)$$

Results and discussion

The results for the hydraulic model

The verification parameter in the model is the roughness coefficient, which changes inversely with water depth. The results of the calibration show that there was little difference between the simulation results and measurements of the discharge and water level at Tan Chau station for two periods from 5/7/1999 to 30/12/1999 (Fig. 6). The graphical results during calibration indicated an adequate calibration and validation over the range of discharges and water levels. However, the calibration results of water level showed a better match than that of discharge. The NSE values for the discharge and water level calibration reached 0.71 and 0.81, respectively, while the R^2 values were 0.82 and 0.88, respectively. According to Moriasi, et al.'s research (2015) [32], these values indicate that the hydraulic model performance peaked very well. It is believed that if a hydrodynamic model is well calibrated, then the predicted results are close to the actual water movements.

The roughness coefficient was recorded after calibration with a range of 0.055 from 0.005 to 0.06 corresponding to water depths from 41 to 0.1 m. During the experimental process, the n_2 (0.003) corresponding to h^2 (25 m) was found to make the roughness coefficient in the study area more suitable for simulation. If $h_{min} < h_{i,j} < h^2$, Eq. (10) is used to calculate the roughness value at a position i,j, while Eq. (11)

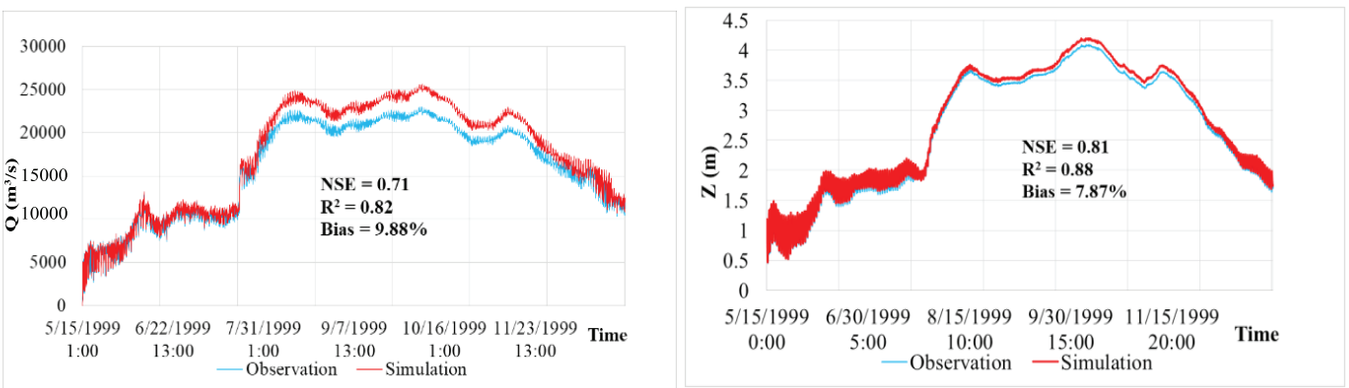

Fig. 6. Calibration results at Tan Chau station from 5/7/1999 to 30/12/1999 for water level (Z) and discharge (Q).

is used when $h_2<h_{i,j}<h_{max}$. These equations are computed as follows:

$$n_{i,j} = \frac{(n_2 - n_{min})(h_{i,j} - h_{min})}{h_2 - h_{min}} + n_{min} \quad (10)$$

$$n_{i,j} = \frac{(n_{max} - n_2)(h_{i,j} - h_2)}{h_{max} - h_2} + n_2 \quad (11)$$

Below is a rough map for the first 500 h starting on 5/15/1999 in Fig. 7. Consequently, the roughness coefficient in the domain is computed according to Eqs. (10) and (11).

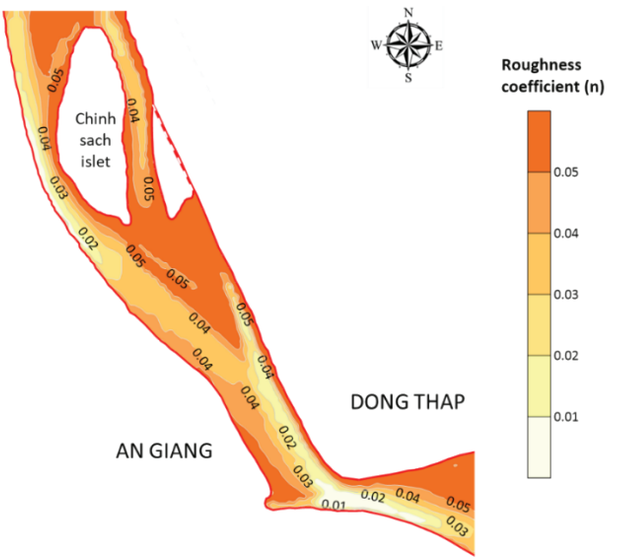

Fig. 7. Roughness coefficient for the study area.

After calibration, the model was validated from 29/06/2001 to 30/12/2001 (flood season). Although the calibration result of the water level showed a better match than discharge (Fig. 8), the evaluation criteria values were satisfactory in terms of both features. The NSE values were 0.71 and 0.81 for discharge and water level, respectively, and the R^2 values were 0.81 and 0.82, respectively. The bias of both the calibration and validation were smaller than 10%.

Calibration and validation results for sediment transport model

Like the hydraulic model, the sediment transport simulation was calibrated and validated for two periods from 5/7/1999 to 30/12/1999 and 29/06/2001 to 30/12/2001. According to the evaluation criteria values, the sediment transport model worked very well in terms of sediment concentration. For calibration and validation, the NSE values were 0.82 and 0.80, respectively, and the R^2 value was 0.91 for both processes. The bias of both calibration and verification was smaller than 10%. Graphical results during calibration and validation at Tan Chau station are shown in Fig. 9.

After calibration and validation, numerous studies have applied bed parameters such as dispersion, critical shear stress for deposition, and acute shear stress for the erosion of bed layers to simulate the processes of sediment transportation, erosion, and deposition [33]. In this study, these parameters were used for calibrating the sediment

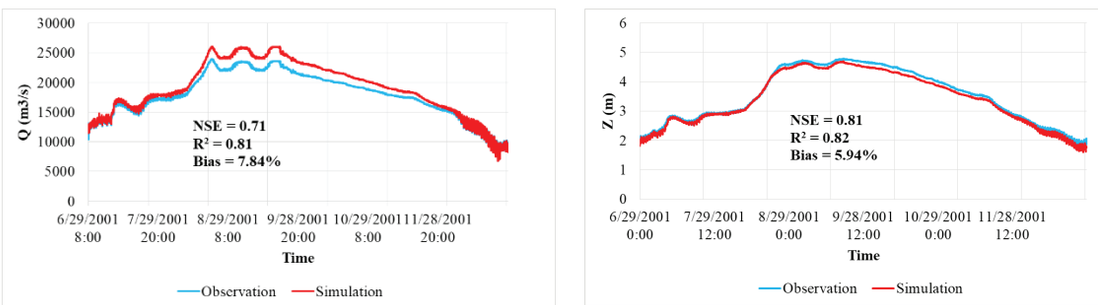

Fig. 8. Observed and simulated data at Tan Chau station from 29/06/2001 to 30/12/2001 for water level (Z) and discharge (Q).

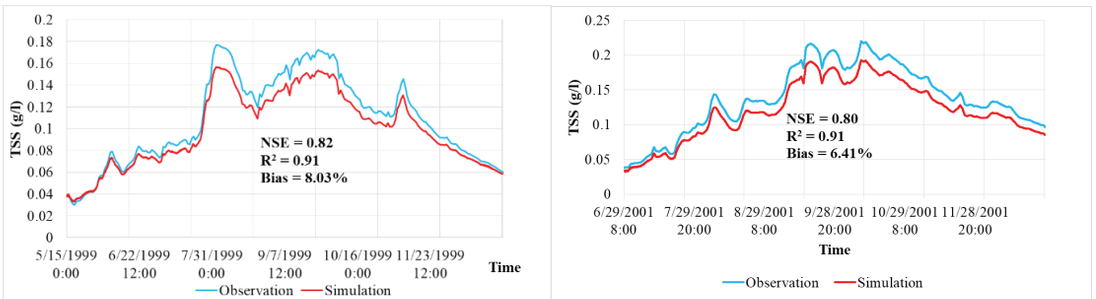

Fig. 9. Observed and simulated TSS data at Tan Chau station for calibration and validation.

simulation and the most relevant parameters in the model are summarized in Table 2.

Table 2. Model parameters.

Parameter	Value
Time step (Δt)	2 s
Mean diameter of particle (D)	0.01 mm
Diameter of particle 90% of the mass of particles present (D_{90})	0.04 mm
Density of particles (ρ_s)	2600 kg/m^3
Kinematic viscosity coefficient (ν)	1.01x10^{-6} m^2/s
Critical shear stress for deposition (τ_d)	0.35 N/m^2
Critical shear stress for erosion (τ_e)	0.04 N/m^2

Simulating bed change of a Tien river segment in Mekong delta from 1999 to 2006

Because the dry season results did not significantly change, we decided to calculate the change in the current study area for the flood seasons from 1999 to 2006. The calculation results of bed changes after each year are extracted and represented by the images shown in Figs. 10 and 11. When applying the moving boundary, the development of mudflats and the loss and formation of islets are calculated.

For example, the Beo islet was an underground islet, with a mesh in the model bathymetry, that eroded from 1999 to 2005 and disappeared in 2006. The model investigated the conditions of the dry/wet cell as described in the methodology. For cells with a depth less than 0.1 m, the model closed the cells and considered them as a dry cell. Then, the simulation results showed the accretion areas over the years. According to the results, the tail of Chinh Sach Islet was deposited over the years including the accretion area. The information is described in more detail in Table 3.

On Dong Thap side, a mudflat area at the downstream site developed from the end of 1999 to 2006. Specifically, the area of the mudflat in 1999 was about 76 hectares and by 2006 the area of the mudflat increased to just over 226 hectares, which is an increase of about 150 hectares compared to 2005, as detailed in Table 3.

Table 3. Increasing mudflat area of simulation.

	2000	2001	2002	2003	2004	2005	2006
A mudflat of Chinh Sach islet tail (m^2)	0.10	0.67	0.16	0.24	0.30	0.14	0.46
A mudflat on Dong Thap province side	1.46	1.01	0.80	0.89	0.76	0.26	0.27

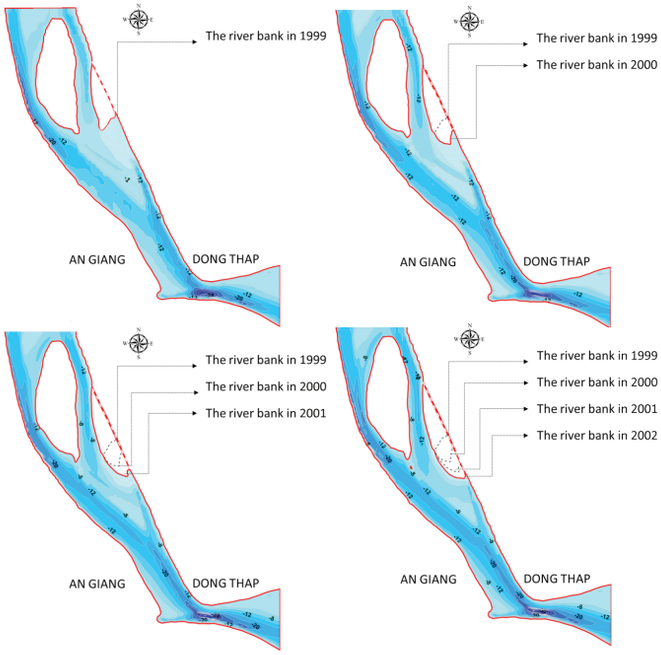

Fig. 10. The bed changes from 1999 to 2002.

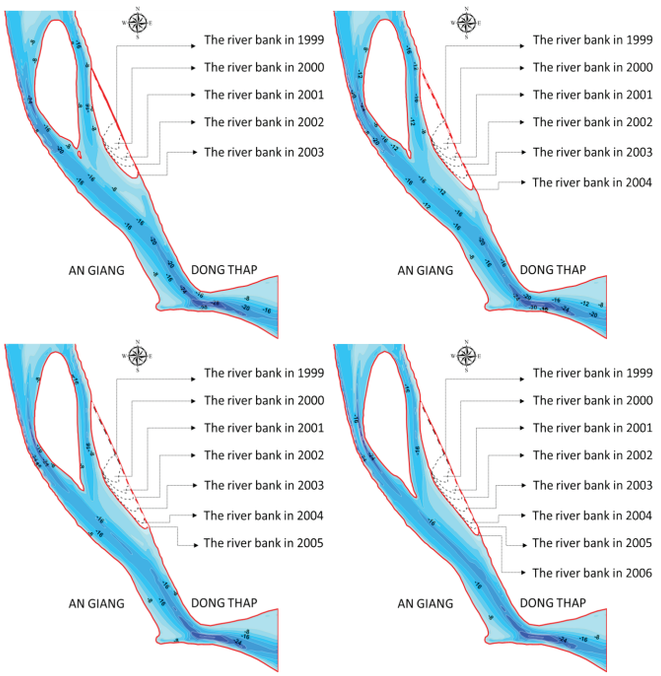

Fig. 11. The bed changes from 2003 to 2006.

The calculation results from the mud flats and Beo islet changes were relatively consistent with the results extracted from Google Earth (GE). The mudflat on the Dong Thap site has grown gradually downstream and the Beo islet has also disappeared in 2006. The tail of the Chinh Sach islet showed gradual expansion downstream (Fig. 12).

Fig. 12. The riverbank from 1999 to 2006 (Source: Google earth).

In the model's study area, the water depth at several cross sections were extracted to record the values each year from 1999 to 2006 at 3 locations denoted cross sections 1, 2, and 3 as described in Fig. 13.

At cross section 1 (Fig. 13) of the model along the bottom left range of the river (on the Dong Thap province side), the bed changes are consistent with the actual bed movements from 1999 to 2006. Specifically, in 1999, the water depth reached an elevation of nearly -18.2 m and gradually accrued to -4.8 m in 2006. The measurement results of the elevation at this area in 2006 was actually -2.1 m. Meanwhile, on the right side of the river (the An Giang province side), there was a gradual erosion trend from -10.8 m in 1999 to -20.9 m in 2006. This trend was also consistent with actual measurements. However, the measurement results showed that the bottom was more eroded and skewed towards the An Giang province. During the data collection, we discovered that there was a sand mine from 2002 to 2004, which made the bed river more eroded in this area compared with the calculation results. It should be noted that the mathematical model in this study did not consider bed change due to sand mining.

In the downstream area, both the Dong Thap and An Giang provinces have built embankments along the river and were not affected by sand mining activities. The simulation results of this downstream area are quite suitable for measurement data. In Fig. 13, there was a variation of the bottom in 2002 where a deep pool was filled with 14 m [34], so the elevation of the deep pool was raised to -28 m (described by dash-dot line in Fig. 13). The deep pool tended to erode again after a period of 4 years from 2003 to 2006. The bed elevation of the deep pool in 2006 was near -38 m while the measurement was actually -36 m at cross section 2 (Fig. 13). At cross-section 3 (Fig. 13), the results do not differ much between simulation and observation. At this position, close to the downstream boundary, the result is satisfactory when applying the characteristic line method. The difference between the simulation and observation was 9.2%.

Conclusions

According to the simulation analyses, we deduce that the HYDIST model well simulates both hydraulic and bed change in the river. For the hydraulic module, the results from the calculated flow and water level models showed high reliability during the process of calibration and validation. The NSE values were 0.71 and 0.81 for discharge and water level, respectively, while the R^2 values were 0.82 and 0.88, respectively. For the sediment transport module, the model performed very well in terms of sediment concentration for calibration and validation, with NSE values of 0.82 and 0.80, respectively, and an R^2 value of 0.91 for both processes. For verification of the model's applicability in a segment of the Tien river, the results were not much different between the simulation and measurement from 1999 to 2006, the percent of difference (BIAS)>10%. The changes of the islets and mudflats were closely modelled to the actual development i.e. the disappearance of Beo and the change in the mudflats on the An Giang side. Furthermore, when extracting the simulation data in some sections, the calculation results were entirely consistent with the actual development. At this position, close to the downstream boundary, the result was still satisfactory when applying the characteristic line method and the difference of comparison between simulation and observation was 9.2%.

However, the bed change module was run without the influence of sand mining in this study. In future studies, sand mining sources will be integrated into the bed load continuity equation.

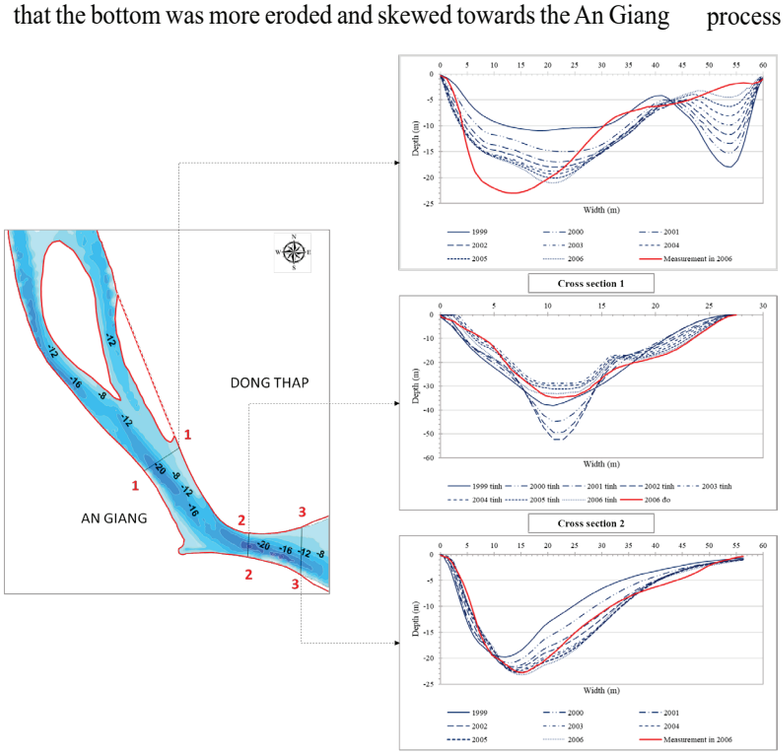

Fig. 13. The water depth at three cross sections.

Nomenclatures

u : depth-averaged horizontal velocity components in x direction (m/s)

v : depth-averaged horizontal velocity components in y direction (m/s)

ς : fluctuation of water surface, compare to "zero" level (m)

H : static depth from the still water surface to the bed (m)

K : friction bed coefficient

A : eddy horizontal viscosity coefficient (m^2/s)

g : acceleration gravity (m/s^2)

C : depth-averaged concentration of suspended load (m^3/m^3)

K_x : dispersion coefficient in Ox direction (m^2/s)

K_y : dispersion coefficient in Oy direction (m^2/s)

H : averaged depth used in the model (H=h+ς) (m)

γ_v : velocity coefficient in the depth; calculated from $\gamma_v = \dfrac{(1-Z)\left[1-\left(\dfrac{a}{H}\right)^{0.2}\right]}{(1.2-Z)\left[1-\left(\dfrac{a}{H}\right)^{1-Z}\right]}$

Z : suspension number and defined after Van Rijn (1993), $Z = \dfrac{\omega_s}{\chi(u_* + 2\omega_s)}$

χ : von Karman constant = 0.4

u_* : bed shear velocity, $u_* = \sqrt{\dfrac{g}{Ch^2}(u^2+v^2)}$

Ch : chezy coefficient, $Ch = 18\log\left(12\dfrac{H}{K_s}\right)$

K_s : bed roughness, $K_s = 3D_{90}$

D_{90} : diameter of particle that is equal to or less than 90% of the mass of particles present

S : standing for erosion and deposition rates (m/s).

M : sediment size-depended coefficient after Van Rijn (1993): 0.00001 ($kg/m^2/s$)

C_b : concentration of bed load (m^3/m^3)

ω_{sm} : particle fall velocity in mixture of water and sediment (m/s), $\omega_{sm} = (1-C)^4\,\omega_s$

ω_s : particle fall velocity, $\omega_s = \dfrac{(\frac{\rho_s}{\rho}-1)gd^2}{18\nu}$

D : mean diameter of particle (m)

ν : kinematic viscosity coefficient (m^2/s)

τ_e : critical bed shear stress for erosion at bottom (N/m^2)

τ_d : critical bed shear stress for deposition at bottom (N/m^2)

τ_b : bed shear stress (N/m^2), $\tau_b = \dfrac{1}{8}\rho f_w V^2$

f_w : friction coefficient of Darcy – Weisbach, calculated from Chezy formula; $f_w = \dfrac{8gn_r^{\,2}}{H^{1/3}}$

ρ : mass density of water (kg/m^3)

ρ_s : density of particles (kg/m^3)

n_r : roughness coefficient

ε_p : void ratio of sediment

D_* : dimensionless particle parameter: $D_* = d_m \left[\frac{g\left(\frac{\rho_s}{\rho} - 1\right)}{\nu^2} \right]^{\frac{1}{3}}$

T : dimensionless bed shear stress: $T = \left[\frac{u_*^2 - u_{*,cr}^2}{u_{*,cr}^2} \right]$

$u_{*,cr}$: critical depth-averaged flow velocity based on Shields (m/s), $u_{*,cr} = 0.25(\frac{\rho_s}{\rho} - 1)^{\frac{8}{15}} d^{\frac{9}{15}} g^{\frac{8}{15}} \nu^{-\frac{1}{15}}$

qb : bed load

$$q_b = 0.053(\frac{\rho_s}{\rho} - 1)g)^{0.5} d_m^{1.5} T^{2.1} D_*^{-0.3} \frac{(u, v)}{\sqrt{u^2 + v^2}}$$

ACKNOWLEDGEMENTS

This research was funded by the Institute for Computational Science and Technology, with the topic "Development of bank erosion numerical model basing on HPC in connection with hydraulic model and to apply for some river reaches of the Mekong river", code No. NDT.28. KR/17.

This work was supported by the Domestic Master/ PhD Scholarship Programme of Vingroup Innovation Foundation.

COMPETING INTERESTS

The authors declare that there is no conflict of interest regarding the publication of this article.

REFERENCES

[1] W.H. Graf (1984), *Hydraulics of Sediment Transport*, Water Resources Publication, 524pp.

[2] L.C. Van Rijn (1984a), "Sediment transport, part I: bed load transport", *Journal of Hydraulic Engineering*, **110(10)**, pp.1431-1456.

[3] L.C. Van Rijn (1984b), "Sediment transport, part II: suspended load transport", *Journal of Hydraulic Engineering*, **110(11)**, pp.1613-1641.

[4] N. Chien and Z. Wan (1999), *Mechanics of Sediment Transport*, ASCE Press, 913pp.

[5] S.I. Khassaf and S.M. Ressen (2014), "Estimation the quantity of sediment transport upstream of Al-Hafar regulator using different formulas", *International Journal of Scientific & Engineering Research*, **5(7)**, pp.456-466.

[6] S.U. Choi and J. Lee (2015), "Prediction of total sediment load in sand-bed rivers in Korea using lateral distribution method", *Journal of the American Water Resources Association*, **51(1)**, pp.214-225.

[7] T. Falkowski, et al. (2017), "Channel morphology changes and their relationship to valley bottom geology and human interventions; a case study from the Vistula valley in Warsaw, Poland", *Geomorphology*, **297**, pp.100-111.

[8] R.G. Jackson (1975), "Velocity-bed-form-texture patterns of meander bends in the lower Wabash river of Illinois and Indiana", *Geological Society of America Bulletin*, **86(11)**, pp.1511-1522.

[9] J. Sun, L. Binliang, Y. Haiyan (2015), "Development and application of a braided river model with non-uniform sediment transport", *Advances in Water Resources*, **81**, pp.62-74.

[10] S. Peirce, P. Ashmore, P. Leduc (2018), "The variability in the morphological active width: results from physical models of gravel-bed braided rivers", *Earth Surface Processes and Landforms*, **43(11)**, pp.2371-2383.

[11] S. Ikeda, M. Yamasaka, M. Chiyoda (1987), "Bed topography and sorting in bends", *Journal of Hydraulic Engineering*, **113(2)**, pp.190-204.

[12] S. Ikeda, G. Parker (1989), "Sediment transport and sorting at bends", *River Meandering*, **12**, pp.103-125.

[13] Z.L. Wei, L.K. Zhao, X.P. Fu (1997), "Research on mathematical model for sediment in Yellow river", *Journal of Wuhan University Hydraulic & Electric Engineering*, **30(5)**, pp.21-25.

[14] W. Wu (2008), *Computational River Dynamics*, CRC Press, 508pp.

[15] L.X. Luu, S. Egashira, H. Takebayashi (2004), *Investigation of Tan Chau Reach in lower Mekong Using Field Data and Numerical Simulation*, Proceedings of Hydraulic Engineering, DOI: 10.2208/prohe.48.1057.

[16] D.H. Zhao, et al. (1994), "Finite-volume two-dimensional unsteady-flow model for river basins", *Journal of Hydraulic Engineering*, **120(7)**, pp.863-883.

[17] P.A. Sleigh, et al. (1998), "An unstructured finite-volume algorithm for predicting flow in rivers and estuaries", *Computers & Fluids*, **27(4)**, pp.479-508.

[18] P. Brufau, P. García-Navarro, M.E. Vázquez-Cendón (2004), "Zero mass error using unsteady wetting - drying conditions in shallow flows over dry irregular topography", *International Journal for Numerical Methods*, **45(10)**, DOI: 10.1002/fld.729.

[19] X. Liu, A. Mohammadian, J.A.I. Sedano (2014), "A well-balanced 2-D model for dam break flow with wetting and drying", *Journal of Fluid Flow, Heat and Mass Transfer*, **1**, pp.30-37.

[20] N.T. Bay, et al. (2019), "HYDIST model and the approach of solving sediment concentration at open boundaries", *Vietnam Journal of Hydro-Meteorology*, **704**, pp.57-64.

[21] N.T. Bay, et al. (2012), "Numerical investigation on the sediment transport trend of Can Gio coastal area (southern Vietnam)", *Journal of Marine Environmental Engineering*, **9(3)**, pp.191-211.

[22] Y. Zhang (2001), *CCHE2D: Two-Dimensional Hydrodynamic and Sediment Transport Model for Unsteady Open Channel Flows Over Loose Bed*, Technical Report No. NCCHE-TR-2001-1, University of Mississippi, 182pp.

[23] T.P. Hoanh (2014), "Current situation of erosion on Tien river bank running through Dong Thap province in the period of 2009-2013", *Journal of Science*, **58**, pp.161-171.

[24] N.T.D. Thuy, et al. (2019), *Modelling Accresion and Erosion Processes in the Bassac and Mekong Rivers of the Vietnamese Mekong Delta*, International Conference on Asian and Pacific Coasts, pp.1431-1437.

[25] D.N. Khoi, et al. (2020), "Morphological change assessment from intertidal to river-dominated zones using multiple-satellite imagery: a case study of the Vietnamese Mekong delta", *J. Regional Studies in Marine Science*, **34**, DOI: 10.1016/j.rsma.2020.101087.

[26] M. Guidolin, et al. (2013), "Using high performance techniques to accelerate demand-driven hydraulic solvers", *Journal of Hydroinformatics*, **15(1)**, pp.38-54.

[27] E.J. Anthony, et al. (2015), "Linking rapid erosion of the Mekong river delta to human activities", *Scientific Reports*, **5(1)**, pp.1-12.

[28] N.T. Bay and M.Q. Trang (2006), "Mathematical model of cohesive sediment transport in the shallow sea basin", *Journal of Science and Technology Development - Vietnam National University, Ho Chi Minh city*, **9**, pp.31-39.

[29] J. Douglas, Jim (1955), "On the numerical integration of by implicit methods", *Journal of the Society for Industrial and Applied Mathematics*, **3(1)**, pp.42-65.

[30] J.E. Nash and J.V. Sutcliffe (1970), "River flow forecasting through conceptual models part I - a discussion of principles", *Journal of Hydrology*, **10(3)**, pp.282-290.

[31] D.N. Moriasi, et al. (2007), "Model evaluation guidelines for systematic quantification of accuracy in watershed simulations", *Transactions of the ASABE*, **50(3)**, pp.885-900.

[32] D.N. Moriasi, et al. (2015), "Hydrologic and water quality models: performance measures and evaluation criteria", *Transactions of the ASABE*, **58(6)**, pp.1763-1785.

[33] A.J. Mehta, et al. (1989), "Cohesive sediment transport. I: process description", *Journal of Hydraulic Engineering*, **115(8)**, pp.1076-1093.

[34] H.Q. Hai (2011), "Correlation of sedimentation - erosion in Tien and Hau rivers", *Journal of Earth Sciences*, **33(1)**, pp.37-44.